 doi:10.20944/preprints202006.0370.v1

Defining and computing reproduction numbers to monitor the outbreak of Covid-19 or other epidemics

Paulo R. Zingano, Janaína P. Zingano,
Institute of Mathematics and Statistics
Universidade Federal do Rio Grande do Sul
Porto Alegre, RS 91509-900, Brazil

Alessandra M. Silva
Companhia de Planejamento do Distrito Federal
Governo de Brasília
Brasília, DF 70620-080, Brazil

AND

Carolina P. Zingano,
School of Medicine
Universidade Federal do Rio Grande do Sul
Porto Alegre, RS 90035-003, Brazil

Abstract

We discuss the generation of various *reproduction ratios* or *numbers* to monitor the outbreak of Covid-19 or other epidemics and examine the effects of intervention/relaxation measures. A detailed SEIR algorithm is described for their computation, with applications given to the current Covid-19 outbreaks in several countries in America (Argentina, Brazil, Mexico, US) and Europe (France, Italy, Spain and UK). The corresponding *matlab script*, complete and ready to use, is provided for free downloading.

Key words: Covid-19 outbreak, SARS-Cov-2 coronavirus, reproduction numbers, deterministic SEIR models, parameter determination, robust methods

AMS Subject Classification: 92-04 (primary); 92-08, 92-10 (secondary)

Matlab code: A complete MATLAB SOURCE CODE to compute reproduction numbers of Covid-19 or other epidemics is freely available by clicking here: find_Rt.m.

Preprints (www.preprints.org) | NOT PEER-REVIEWED | Posted: 30 June 2020 doi:10.20944/preprints202006.0370.v1

1. Introduction

The monitoring of the evolving state of a serious epidemic can be done during and after its outbreak by estimating the daily values of basic ratios generally known as reproductive or reproduction numbers [5, 6, 7, 13]. While not properly geared to allow serious predictions of future values of the epidemic, they are nevertheless able to display the past and present history with amazing clarity. However, as their calculation depends on the values of various mathematical parameters (like the length of transmission and incubation periods), this ability may be impaired by inaccuracies in their estimation. This is particularly true for the widely used *basic reproduction number*, which measures the average number of secondary cases generated by a typical infectious individual in a full susceptible population (Figure 1).

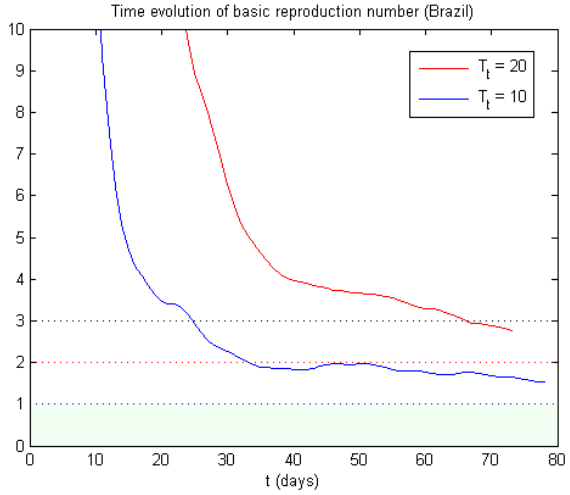

Fig. 1: Time evolution of standard *basic reproduction numbers* of Covid-19 in Brazil since the date of 100 cases reported ($t = 0$), showing the effect of two distinct hypothetical transmission periods ($T_t = 20$ and $T_t = 10$, resp.). In this example, $t = 0$ corresponds to 03/13/2020. (Data source: covid.saude.gov.br)

On the other hand, once some mathematical model has been chosen to simulate the disease dynamics and its parameters determined, several alternative reproductive numbers become automatically available at no additional computational cost, many showing very little dependence on key parameters like transmission or incubation times. We will illustrate this fact in the context of deterministic SEIR models, but our approach can be adapted to other mathematical models (deterministic or stochastic) as well.

The idea is most easily explained by considering the simplest SEIR model of all, defined by the equations (1.1) below. This model divides the entire population in question into four classes: the *susceptible* individuals (class S), those *exposed* (class E, formed by infected people who are still inactive (i.e., not yet transmitting the disease), the *active infected* or *infectious* individuals (class I) and the *removed* ones. The latter class is formed by those who have *recovered* from the disease (class R) or who have *died* from it (class D). The dynamics between the various classes is given in the universal language of calculus by the differential equations

Preprints (www.preprints.org) | NOT PEER-REVIEWED | Posted: 30 June 2020 doi:10.20944/preprints202006.0370.v1

$$\begin{cases} \dfrac{dS}{dt} &= -\beta \dfrac{S(t)}{N} I(t), \\ \dfrac{dE}{dt} &= \beta \dfrac{S(t)}{N} I(t) - \delta E(t), \\ \dfrac{dI}{dt} &= \delta E(t) - (r+\gamma) I(t), \\ \dfrac{dR}{dt} &= \gamma I(t), \\ \dfrac{dD}{dt} &= r I(t), \end{cases} \tag{1.1}$$

see e.g. [2, 4, 7, 12] for a detailed discussion of the various terms and their meanings. The parameters β (AVERAGE TRANSMISSION RATE) and r (AVERAGE LETHALITY RATE of the population I due to the disease) vary with t (time, here measured in DAYS), but δ and γ are typically positive constants given by

$$\gamma = \frac{1}{T_t}, \qquad \delta = \frac{1}{T_i}, \tag{1.2}$$

where T_t denotes the AVERAGE TRANSMISSION PERIOD and T_i stands for the MEAN INCUBATION TIME, which will be taken as 14 and 5.2, respectively [9, 10, 14]). In the system (1.1), N denotes the full size of the susceptible population initially exposed, so that we have $S(t_0) + E(t_0) + I(t_0) + R(t_0) + D(t_0) = N$, where t_0 denotes the initial time. Observing that, by the equations (1.1), the sum $S(t)+E(t)+I(t)+R(t)+D(t)$ is invariant, it follows the CONSERVATION LAW

$$S(t) + E(t) + I(t) + R(t) + D(t) = N, \qquad \forall\ t > t_0, \tag{1.3}$$

since, for simplicity, the model neglects any changes in the population due to birth, migration or death by other causes during the period of the epidemic (of the order of a few months). To well define the model (1.1), besides informing the functions $\beta(t)$ and $r(t)$ we need to provide the initial values $S(t_0)$, $E(t_0)$, $I(t_0)$, $R(t_0)$, $D(t_0)$, which is not a trivial task, since not all of these variables are reported, and those reported may be in error — which may well be large in case of significant underreporting.

It thus seems clear that predicting reasonably right values for the variables $S(t)$, $E(t)$, $I(t)$, $R(t)$ and $D(t)$ at future times is *not* a simple problem, especially in the long time range. The situation becomes even more complicated for more complex (i.e., stratified) models, which add other variables and parameters to be determined. Calibrating many parameters can quickly become a nightmare. For all its simplicity, models with few variables and parameters like (1.1) can yield surprisingly good results and thus should not be overlooked, as will be seen in the sequel.

Preprints (www.preprints.org) | NOT PEER-REVIEWED | Posted: 30 June 2020 doi:10.20944/preprints202006.0370.v1

2. Implementing the SEIR model

Having introduced the SEIR equations (1.1), we now describe an implementation of this model that is suitable for the computation of reproduction numbers.

(*i*) *assigning a value to the population parameter* N

In the case of Covid-19, which can be considered a new virus (SARS-CoV-2), it has been common to assume the entire population susceptible and assign its whole value to N. This is highly debatable, since this parameter refers to that particular fraction of the susceptible population that is effectively subject to infection. For deterministic models, this introduces the possibility that an outbreak might *not* happen after the introduction or reintroduction of a few infected individuals, as it has been long recognized in the stochastic literature [1, 9]. In any case, it turns out that N is not so much important for the short range dynamics as it proves to be in the long run (see Figures 2*a* and 2*b*), so that for our present purposes this is not a serious issue. We have therefore taken for N the full population of the region under consideration.

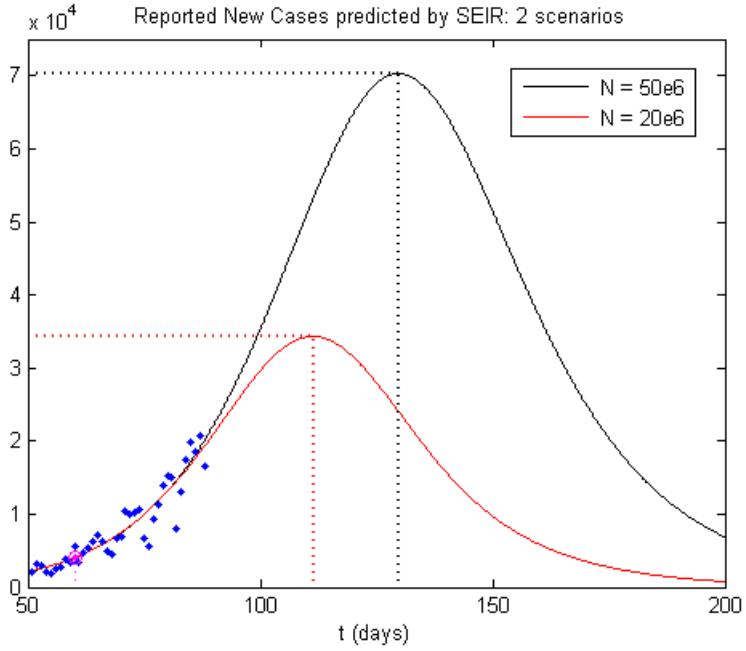

Fig. 2*a*: Prediction by model (1.1) of the daily number of *new cases* of Covid-19 expected to be reported in Brazil between the initial time $t = t_0 = 60$ (April 25th) and $t = 200$ (September 12th), considering susceptible populations of N= 20 million (red curve) and N= 50 million (black curve). Note the appreciable difference between the predicted peak values (34 and 70 thousand, resp.) and their respective dates, June 6th and July 4th. Actual data points are shown in blue. (Computed from data available at the official site https://covid.saude.gov.br.)

Preprints (www.preprints.org) | NOT PEER-REVIEWED | Posted: 30 June 2020 doi:10.20944/preprints202006.0370.v1

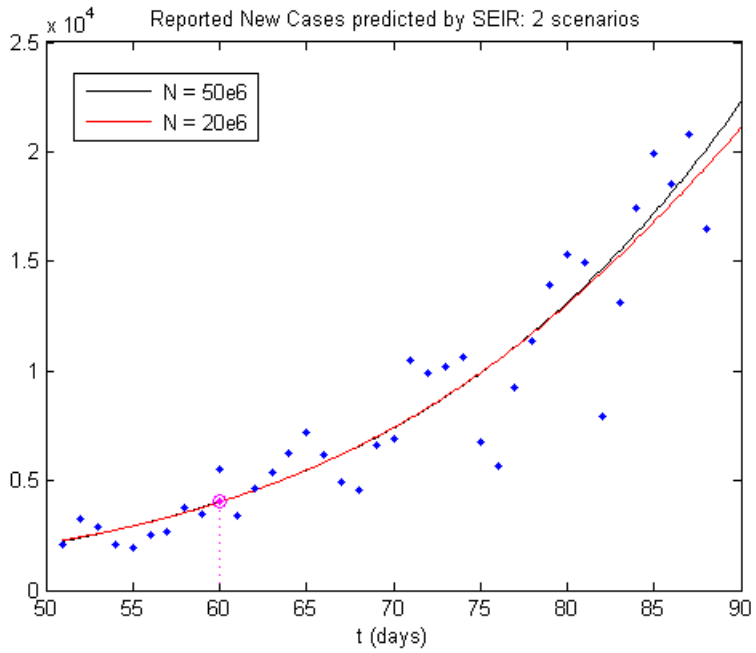

Fig. 2*b*: Thirty day prediction by model (1.1) of the daily number of *new cases* of Covid-19 to be reported in Brazil between the initial time $t = t_0 = 60$ (04/25) and $t = 90$ (05/25), considering susceptible exposed populations of $N = 20$ million (red curve) and $N = 50$ million (black curve). Note the very close similarity of the two 30D predictions in spite of the appreciable difference in the values of N. Points shown in blue are the official values reported (cf. https://covid.saude.gov.br.)

(ii) generation of initial data $S(t_0)$, $E(t_0)$, $I(t_0)$, $R(t_0)$, $D(t_0)$

Initial values S_0, E_0, I_0, R_0, D_0 for the five variables are generated from a starting date t_s on, which is taken so as to meet some minimum value chosen of total reported cases (typically, 100). Denoting by $C_r(t)$ the total amount of reported cases up to some time t, and letting $\mathrm{EIR}(t)$ be the sum of the populations $E(t)$, $I(t)$ and $R(t)$, we set

$$\mathrm{EIR}(t_s) \;=\; f_c \cdot (C_r(t_s) - D(t_s)), \tag{2.1}$$

where $f_c \geq 1$ denotes a CORRECTION FACTOR to account for likely underreportings on the official numbers given. (In (2.1), we have neglected possible underreportings on the number of deaths, which could of course be similarly accounted for if desired.) Again, this factor will not play an important role in this paper and could be safely ignored, but it should be carefully considered in the case of long time predictions. Having estimated $\mathrm{EIR}(t_s)$, we then set

$$E(t_s) \;=\; E_0(t_s) := \; a \cdot (1-b) \cdot \mathrm{EIR}(t_s), \tag{2.2a}$$

$$I(t_s) \;=\; I_0(t_s) := \; (1-a) \cdot (1-b) \cdot \mathrm{EIR}(t_s), \tag{2.2b}$$

Preprints (www.preprints.org) | NOT PEER-REVIEWED | Posted: 30 June 2020 doi:10.20944/preprints202006.0370.v1

$$R(t_s) \;=\; R_0(t_s) := \; b \cdot \mathrm{EIR}(t_s), \tag{2.2c}$$

$$S(t_s) \;=\; S_0(t_s) := \; N - \big(E(t_s) + I(t_s) + R(t_s) + D(t_s)\big), \tag{2.2d}$$

where $a = T_i/(T_i + T_t)$ and $b = 0.30$, consistently with the literature (see e.g. [14]). The arbitrariness in this choice of weights gets eventually corrected as we compute more values $S_0(t_0), E_0(t_0), I_0(t_0), R_0(t_0), D_0(t_0)$ at later initial times $t_0 = t_s + 1, ..., t_{_F}$, where $t_{_F}$ stands for the final (i.e., most recent) date of reported data available. For each t_0, the solution of the equations (1.1) with the previously obtained initial data at $t_0 - 1$ is computed on the interval $J(t_0) = [\,t_0 - 1,\, t_1\,]$, $t_1 = \min\{\,t_0 - 1 + d_0,\, t_{_F}\}$, with constant parameters $\beta = \beta_0(t_0 - 1)$, $r = r_0(t_0 - 1)$ determined so that the computed values for $C_r(t)$, $D(t)$ best fit the reported data for these variables on $[\,t_0,\, t_1\,]$ in the sense of LEAST SQUARES [12]. (Here, $d_0 \in [\,2,\, 10\,]$ is chosen according to the data regularity.) Once this solution $(S, E, I, R, D)(t)$ is obtained, we set $S_0(t_0) := S(t_0)$, $E_0(t_0) := E(t_0)$, $I_0(t_0) := I(t_0)$, $R_0(t_0) := R(t_0)$, $D_0(t_0) := D(t_0)$ and move on to the next time level $t_0 + 1$, repeating the procedure until $t_{_F}$ is reached.

(*iii*) *computing the solution on some final interval* $[\,t_0, T\,]$ (PREDICTION PHASE)

Having completed the previous steps, we can address the possibility of *prediction*. Although this is not important for our present goals, it is included for completeness. Choosing an initial time $t_0 \in (t_s,\, t_{_F}]$, we then take the initial values

$$S(t_0) = S_0(t_0),\;\; E(t_0) = E_0(t_0),\;\; I(t_0) = I_0(t_0),\;\; R(t_0) = R_0(t_0),\;\; D(t_0) = D_0(t_0).$$

In order to predict the values of the variables $S(t), E(t), I(t), R(t), D(t)$ for $t > t_0$, it is important to have good estimates for the evolution of the key parameters $\beta(t)$ and $r(t)$ beyond t_0. This is the most computationally intensive part of the algorithm and is better executed in large computers. Such estimates can be given in the form

$$\beta(t) \;=\; \beta_0 \,+\, a_\beta\, e^{-\,\lambda_\beta (t\,-\,t_0)} \tag{2.3a}$$

$$r(t) \;=\; r_0 \,+\, a_r\, e^{-\,\lambda_r (t\,-\,t_0)} \tag{2.3b}$$

where $\beta_0, a_\beta, \lambda_\beta, r_0, a_r, \lambda_r \in \mathbb{R}$ are determined so as to minimize the maximum size of weighted RELATIVE ERRORS in the computed values for $C_r(t), D(t)$ as compared to the official data reported for these variables on some previous interval $[\,t_0 - \tau_0,\, t_0]$ (weighted CHEBYCHEFF PROBLEM) for some chosen $\tau_0 > 0$ (usually, $20 \le \tau_0 \le 30$). This problem is solved iteratively starting with an initial guess obtained from the analysis of the previous values $\beta_0(t), r_0(t)$ computed in the step (*ii*) above. The result is illustrated in Figure 3 for the case of $\beta(t)$, with similar considerations for $r(t)$.

Preprints (www.preprints.org) | NOT PEER-REVIEWED | Posted: 30 June 2020 doi:10.20944/preprints202006.0370.v1

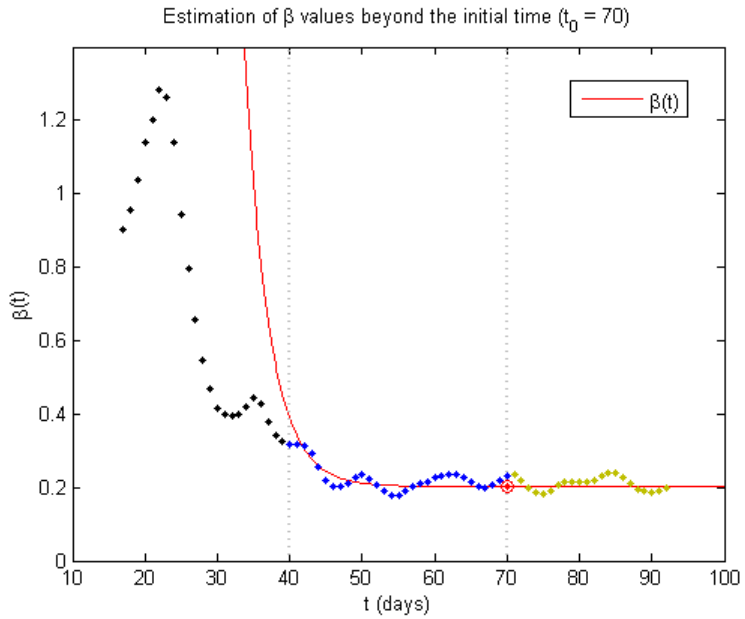

Fig. 3: Estimation of future values of the transmission parameter $\beta(t)$ beyond the initial time $t_0 = 70$ (05/05/2020) for the outbreak of Covid-19 in Brazil, assuming the basic form (2.3a), after solving the Chebycheff problem (red curve). The data points in the interval $[40, 70]$, shown here in blue, are values of the function $\beta_0(t)$ computed in step (ii), which are used to obtain the first approximation to $\beta(t)$. Values of $\beta_0(t)$ previous to $t = 40$ (04/05/2020), shown in black, are disregarded. The golden points beyond $t_0 = 70$ are future values of $\beta_0(t)$, not available on 05/05/2020, displayed to allow comparison with the predicted values $\beta(t)$.

Once $\beta(t)$, $r(t)$ have been obtained, the equations (1.1) are finally solved (Figure 4).

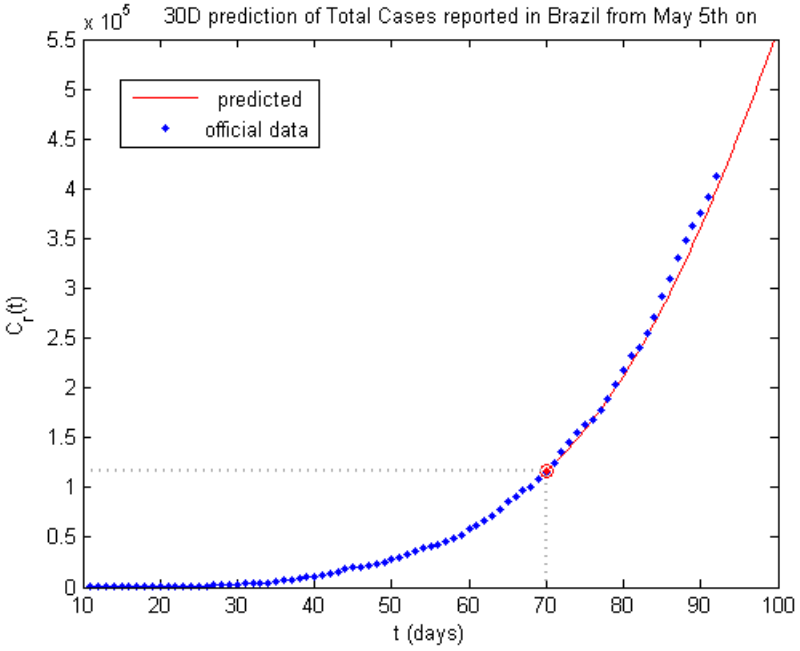

Fig. 4: Computation of $C_r(t) = \big(E(t) + I(t) + R(t)\big)/f_c + D(t)$ for $t > t_0 = 70$ (05/05/2020), with initial data $C_r(t_0) = \big(E_0(t_0) + I_0(t_0) + R_0(t_0)\big)/f_c + D_0(t_0)$, after obtaining $\beta(t)$, $r(t)$ – see Fig. 3 for $\beta(t)$. The numerical solution of equations (1.1) is easily obtained by any method.

Preprints (www.preprints.org) | NOT PEER-REVIEWED | Posted: 30 June 2020 doi:10.20944/preprints202006.0370.v1

3. Reproduction numbers

A natural by-product of the results generated by the algorithm is the estimate of *reproduction numbers* of the epidemic, which measure the intensity of transmission at various times and, in doing so, are useful indicators to monitor the situation and the effects of intervention procedures that may have been taken. Using the generic symbol R_t to denote such quantities,[1] they signal a rise in the number of infections in the case $R_t > 1$, their decrease when $R_t < 1$, and temporary steadiness if $R_t = 1$. For instance, rewriting the equation for the critical population $I(t)$ in the form

$$\frac{dI}{dt} \;=\; \alpha(t)\, I(t), \qquad \alpha(t) := \delta \cdot E(t)/I(t) \,-\, r(t) - \gamma, \tag{3.1a}$$

we see that $I(t)$ will increase if $\alpha(t) > 0$, decrease when $\alpha(t) < 0$ and stay about the same if $\alpha(t) = 0$ — or, in terms of the ratio

$$R_t := \frac{\delta \cdot E(t)/I(t)}{r(t) + \gamma}, \tag{3.1b}$$

whether we have $R_t > 1$, $R_t < 1$ or $R_t = 1$, respectively. Another natural possibility would be to consider basic ratios like

$$R_t := \frac{I(t+d)}{I(t-d)}, \qquad R_t := \frac{E(t+d) + I(t+d)}{E(t-d) + I(t-d)} \tag{3.2}$$

for some chosen $d > 0$. For example, the choice $d = T_t/2$ corresponds to the standard *basic reproduction number*, or the mean number of secondary infections caused by a typical infected individual during his transmission period [9, 12]. The corresponding expressions would be, using the calculations performed in step (ii) of the algorithm,

$$R_t^{(1)} := \frac{\delta \cdot E_0(t)/I_0(t)}{r_0(t) + \gamma}, \tag{3.3}$$

where $r_0(t)$ denotes the lethality rates computed there, or else

$$R_t^{(2)} := \frac{I_0(t+3)}{I_0(t-3)}, \qquad R_t^{(3)} := \frac{E_0(t+3) + I_0(t+3)}{E_0(t-3) + I_0(t-3)}, \tag{3.4}$$

and so forth. These indicators point to similar scenarios (Figure 5), with $R_t^{(1)}$ seemingly more influenced by seasonal (weekly) variations in the data. We have found $R_t^{(2)}$ particularly useful, with numerical results that are consistent with previous analyses

[1] The notation R_t is natural in stochastic models, and is adopted here as we have already used $R(t)$, $R_0(t)$ with other meanings (size of the recovered population and their initial values, resp.).

Preprints (www.preprints.org) | NOT PEER-REVIEWED | Posted: 30 June 2020 doi:10.20944/preprints202006.0370.v1

(see e.g. [13]). For time scales such as those of Covid-19, the choice $d = 3$ is good to zoom in the scenario and facilitate the reading (Figure 6), while not compromising robustness (Figure 7).

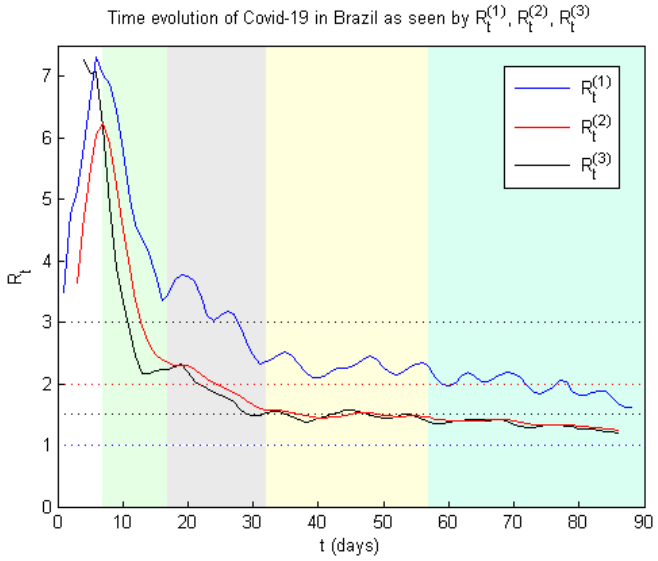

Fig. 5: Comparison of the time evolution of Covid-19 in Brazil (since 100 cases reported) as seen by the indicators defined in (3.3), (3.4), pointing to similar scenarios. In the three cases it is clear that Brazil has not yet reached a state of control of the epidemic ($R_t < 1$)

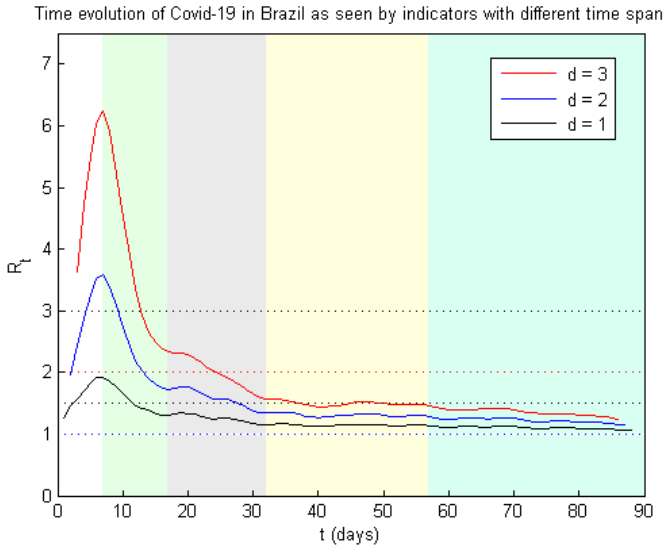

Fig. 6: Comparison of the time evolution of Covid-19 in Brazil (since 100 cases reported) as seen by $R_t = I(t+d)/I(t-d)$ for different values of d, showing similar scenarios. In the three cases it is clear that Brazil has not yet reached a state of control of the epidemic ($R_t < 1$)

Preprints (www.preprints.org) | NOT PEER-REVIEWED | Posted: 30 June 2020 doi:10.20944/preprints202006.0370.v1

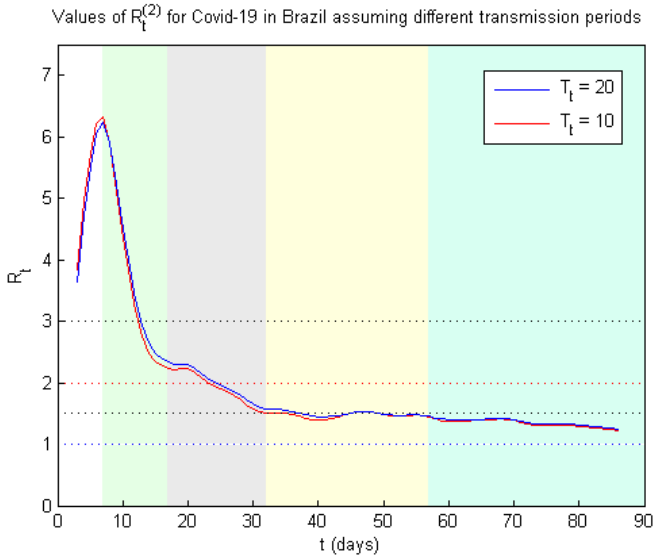

Fig. 7: Robustness of $R_t^{(2)}$ with respect to large uncertainties on the value of transmission time. Date zero refers to 100 cases reported, that is: 03/13/2020. (As in Fig. 5 and Fig. 6 above, calculations were based upon official data reported at https://covid.saude.gov.br.)

4. Applications

In this section we will illustrate the use of reproduction values by examining the evolution of Covid-19 in various countries around the world under the view of such numbers — choosing for definiteness the numeric ratio $R_t^{(2)}$ defined in (3.4) above as our basic indicator, unless explicitly stated otherwise. Thus, we set

$$R_t \;=\; \frac{I_0(t+3)}{I_0(t-3)} \tag{4.1}$$

where $I_0(s)$ is the size of the active infected population at time s as computed in the step (ii) of the SEIR algorithm (see Section 2).

Taking right decisions about intervention or relaxation measures is a very difficult and complex process that involves a careful consideration of various mathematical indicators and a lot of other factors including many health, economic and social issues. In the following examples we consider only the single factor given by reproduction numbers. For all the simplicity and obvious limitations of this approach, it offers nevertheless precious insight and information about the disease dynamics and evolution.

Acknowledgements. In the following examples, the computation of all the curves shown was based on data available for each country at worldometers/coronavirus.

Preprints (www.preprints.org) | NOT PEER-REVIEWED | Posted: 30 June 2020 doi:10.20944/preprints202006.0370.v1

Example 1: Time evolution of Covid-19 in Argentina since 03/18/2020 ($t = 0$), the date of 97 total cases reported. Strong containment measures had begun 3 days earlier ($t = -3$) and managed to keep the number of cases and deaths down low, with R_t decreasing continually until 05/04/2020 ($t = 47$), when it reached a minimum value of 1.08. Following that, the situation deteriorated with R_t increasing to 1.54 on 05/24/2020 ($t = 67$), despite the reinforcement of most intervention procedures. Partial relaxation of some of these measures was introduced on 06/01/2020 ($t = 75$) and, in this new period, R_t has remained relatively stable at 1.30 (yellow band), but tending to slowly increase (present value is 1.32). Bringing the epidemic to a state of nationwide control ($R_t < 1$) still seems far away. This example illustrates the unfortunate fact that having low numbers of infections does not necessarily mean having the epidemic under control.

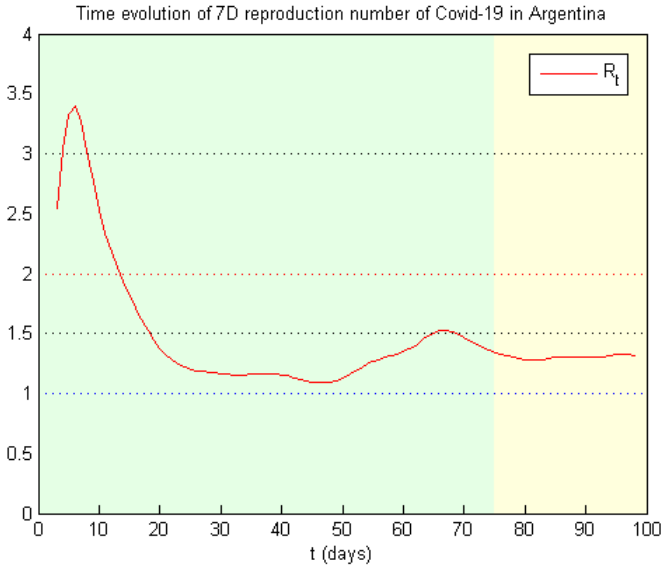

Example 2: Time evolution of Covid-19 in Brazil since 03/13/2020, the date of 98 total cases reported ($t = 0$). With very poor coordination between the central and local authorities and with different levels of intervention in the various states of the country, the decreasing of R_t after reaching 1.5 by mid-April proceeded very slowly (green band) due to the spread of the epidemic and the emergence of new infection foci. Relaxation measures began to be implemented on different dates according to the individual regions, but can be traced on average back to 06/01/2020 ($t = 80$). Despite the encouraging behavior of R_t shown in the following fortnight (yellow band),

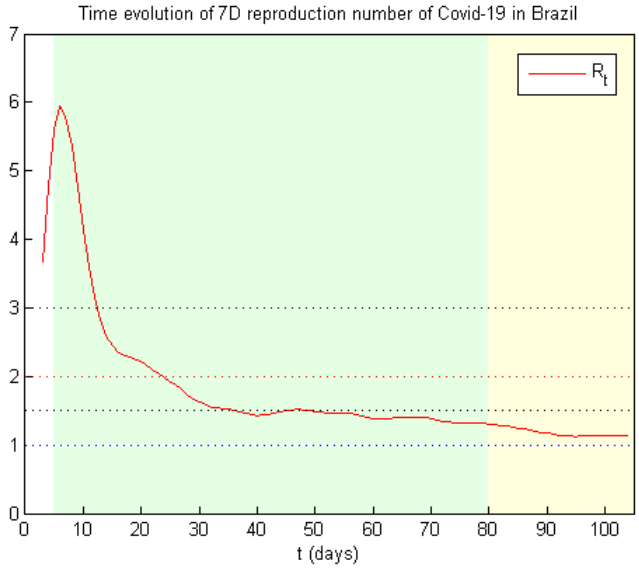

Preprints (www.preprints.org) | NOT PEER-REVIEWED | Posted: 30 June 2020 doi:10.20944/preprints202006.0370.v1

the indicator resumed increasing by mid-June due to further disease development in less affected areas of the country, particularly the southern and central western states. Another negative factor is that flexibilization of control measures has been introduced before the various regions had attained a state of epidemic control ($R_t < 1$), which is *not* ideal.

Example 3: Time evolution of Covid-19 in France since 02/29/2020 ($t = 0$), the date of 100 total cases reported. Containment measures began relatively late on 03/16/2020 ($t = 16$), with a strict eight-week lockdown that reduced the value of R_t down to 0.81 (green band). Restrictions were afterwards relaxed (yellow band), with R_t stable for a couple of weeks, when it began increase. A peak value of 0.99 was reached on 05/30/2020, followed by a reduction to 0.89 on 06/08/2020 ($t = 100$), staying on a slow ascent ever since (its present value is 0.94). The situation requires careful monitoring, with the possibility of having to impose some containment restrictions back to keep the epidemic under nationwide control ($R_t < 1$). Plotting the size of the ACTIVE INFECTED population (i.e., the function $I_0(t)$ computed in the step (ii) of the algorithm, assuming $f_c = 2$), displayed on the right, shows a small resurgent peak by late May ($t = 92$), followed by a slower pace decrease from that moment on.

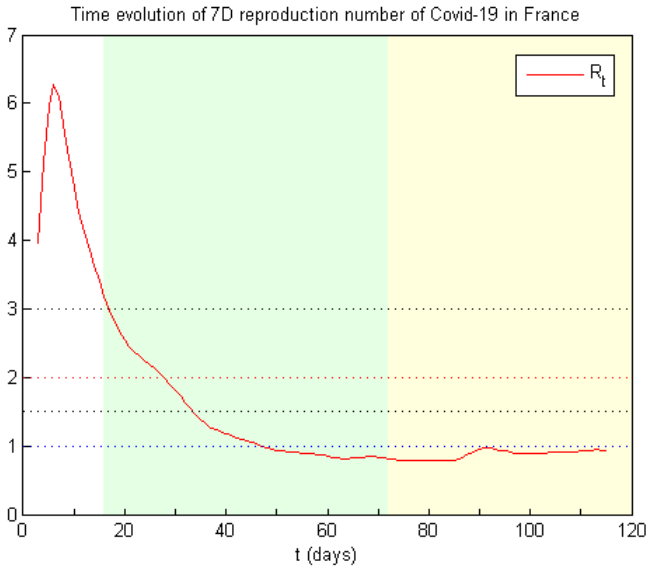

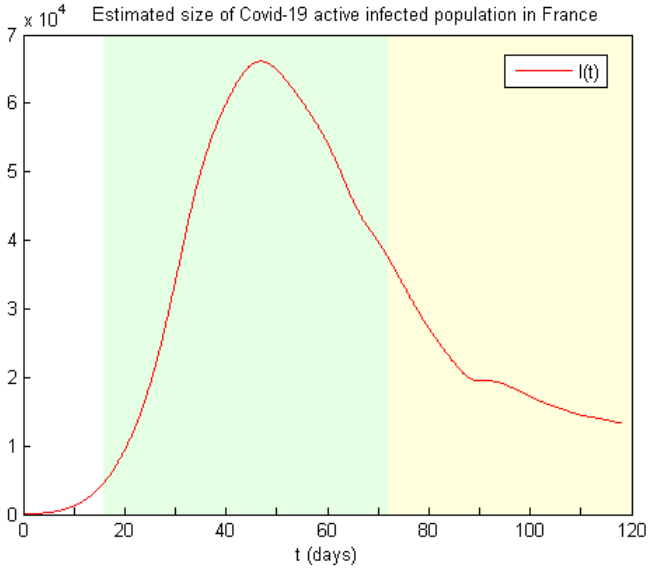

Preprints (www.preprints.org) | NOT PEER-REVIEWED | Posted: 30 June 2020 doi:10.20944/preprints202006.0370.v1

Example 4: Time evolution of Covid-19 in Italy since 02/22/2020, the date of 79 total cases reported ($t = 0$). Containment measures began fifteen days later, with a strict eight-week national lockdown imposed on 03/10/2020 ($t = 17$). The strong intervention, embraced by the population and maintained for the whole period, succeeded in reducing R_t continually down to a safe value of 0.80 on 05/18/2020 ($t = 86$), when some of the contention rules began being relaxed (yellow band). The descent continued for nineteen days, reaching a bottom value of 0.77 on 06/06/2020 ($t = 105$). After this, a steady and very slow increase set in leading to the present value of 0.83 ($t = 123$). The epidemic presently seems very much under control in Italy, with the infected populations (classes E and I) decreasing steadily, as seen by plotting the variables $E_0(t)$, $I_0(t)$ obtained in the step (ii) with $f_c = 2$, shown on the right.

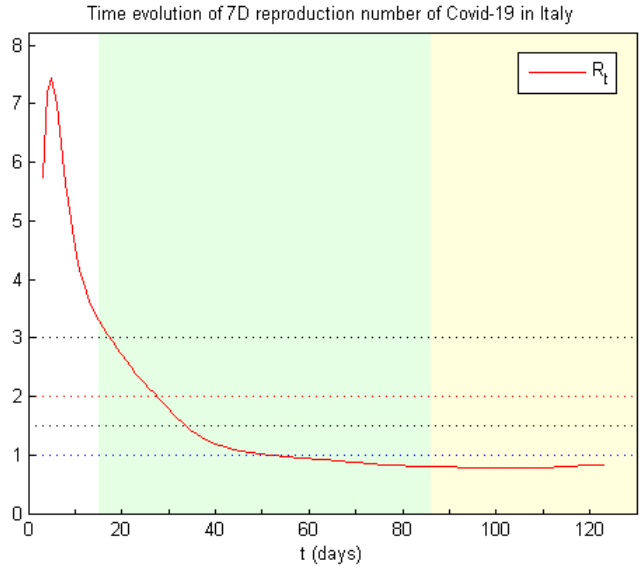

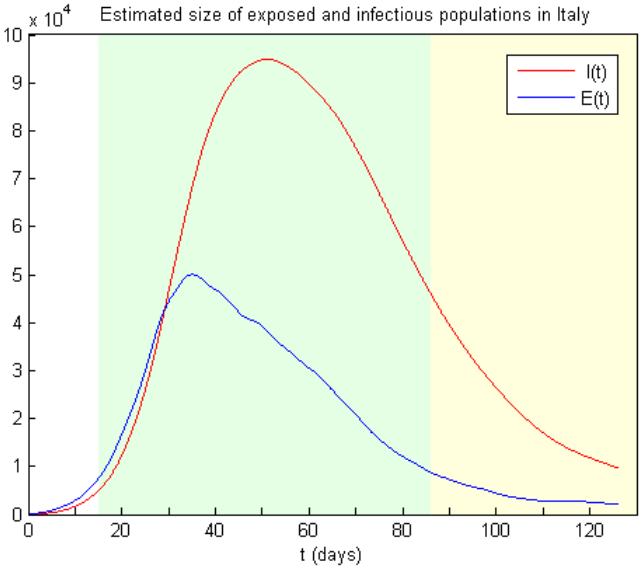

Example 5: Time evolution of Covid-19 in Mexico since 03/18/2020, the date of 93 total cases reported ($t = 0$). After containment measures began on 03/22/2020 ($t = 4$), the value of R_t continually decreased to 1.20 (green band), when restrictions began to be relaxed on 06/01/2020 (yellow band). Relaxation measures have apparently not changed the behavior of R_t afterwards, but reach-

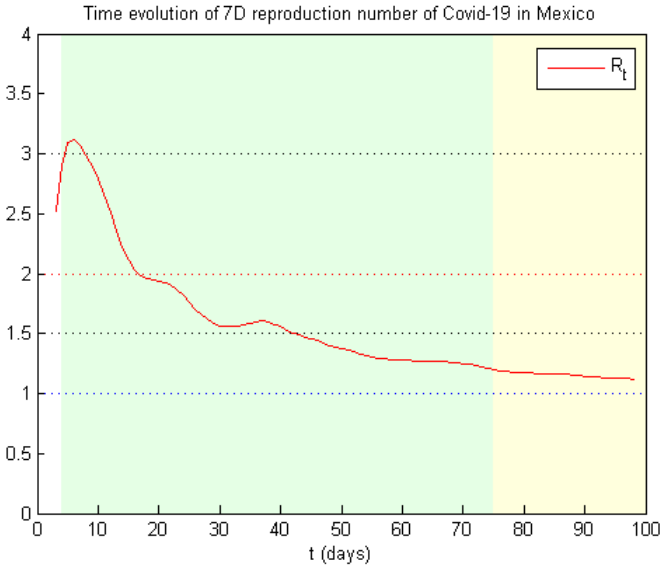

Preprints (www.preprints.org) | NOT PEER-REVIEWED | Posted: 30 June 2020 doi:10.20944/preprints202006.0370.v1

ing a state of control still looks a few weeks away. Similarly to Argentina and Brazil, the flexibilization started before the country had properly entered the safe zone $R_t < 1$.

Example 6: Time evolution of Covid-19 in Spain since 03/01/2020, the date of 84 total cases reported ($t = 0$). After containment measures began on 03/13/2020 ($t = 12$), the value of R_t continually decreased to 0.89 on 05/11/2020 ($t = 71$), when restrictions began to be relaxed (yellow band). A minimum value of 0.75 was finally reached on 06/07/2020 ($t = 98$), after which a slow, steady increase set in towards the present value of 0.83 ($t = 115$), in much the same way as Italy.

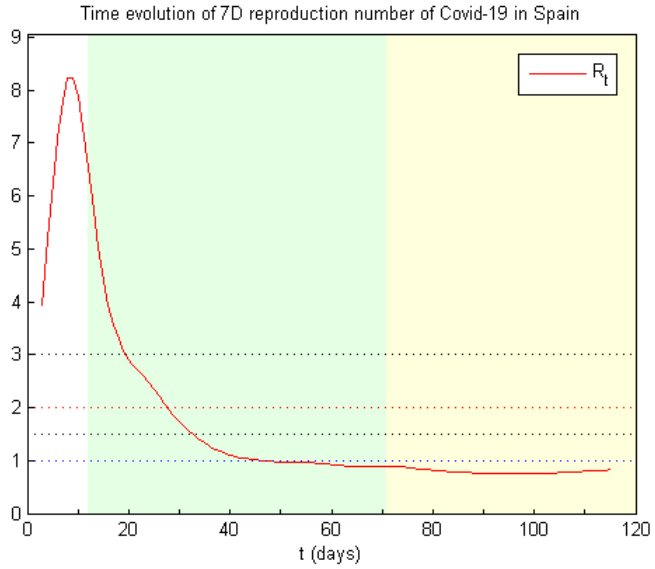

Example 7: Time evolution of Covid-19 in the UK since 03/04/2020, the date of 87 total cases reported ($t = 0$). After containment measures began relatively late on 03/20/2020 ($t = 16$), including strict national lockdown and other rules three days later, the value of R_t continually decreased to 0.98 on 05/13/2020 ($t = 70$), when restrictions began to be relaxed, and then further down to 0.86 nineteen days later, when the lockdown was removed (yellow band). Despite successfully bringing the epidemic under control, the number of reported cases and deaths was very high due to the initial delay in taking intervention action.

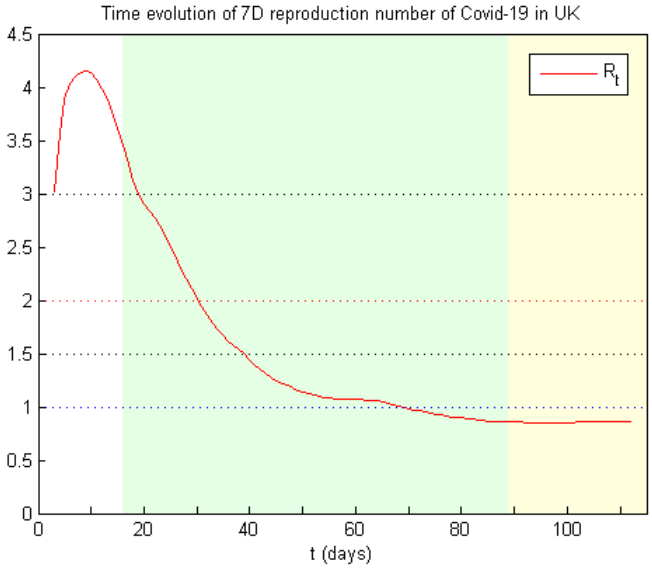

Preprints (www.preprints.org) | NOT PEER-REVIEWED | Posted: 30 June 2020 doi:10.20944/preprints202006.0370.v1

Example 8: Time evolution of Covid-19 in the US since 03/02/2020, the date of 100 total cases reported ($t = 0$). After containment measures began on 03/15/2020 ($t = 13$), R_t successfully decreased continually to 0.97 on 05/15/2020 ($t = 74$), when restrictions began to be relaxed, and then slightly down to 0.96 on 05/27/2020 ($t = 86$), followed by a slow and steady increase to the present value of 1.11 (yellow band). With a poor coordination between central and local authorities in the beginning of the epidemic, the country suffered a high mortality rate (0.0388 %) and number of infections (more than 2.6 million cases reported). As of 06/27/2020, the US have not succeeded in bringing down the epidemic under nationwide control. A second peak ("second wave") in the size of the active infected population is now clear to happen sometime in the future, as indicated by the curve of $I_0(t)$ shown on the right.

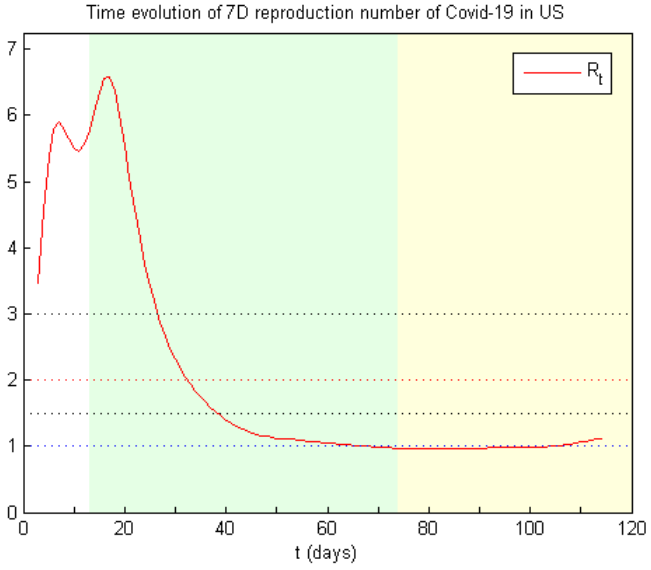

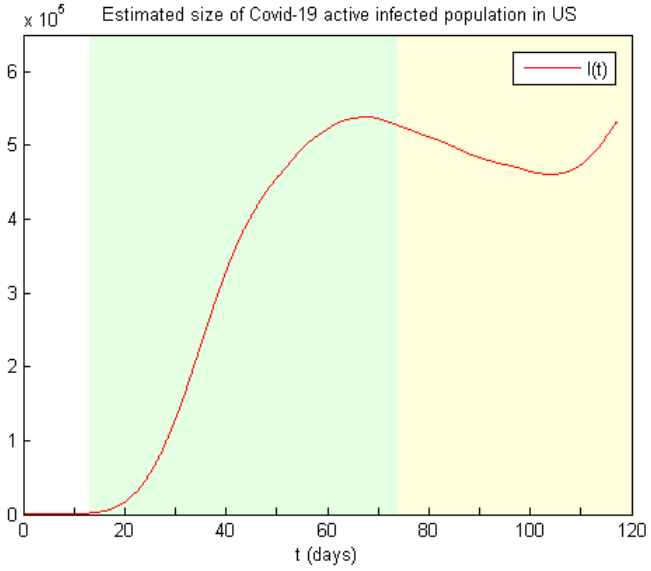

References

[1] L. S. Allen, *An introduction to stochastic epidemic models*, in: F. Brauer et al (Eds), Mathematical Epidemiology, Lecture Notes in Mathematics, vol. 1945, Springer, New York, 2008, pp. 81-130.

[2] F. Brauer, P. van den Driessche and J. Wu (eds), Mathematical Epidemiology, Lecture Notes in Mathematics, vol. 1945, Springer, New York, 2008.

[3] O. Diekmann, J. P. Heesterbeek and J. J. Metz, *On the definition and the computations of the basic reproduction ratio R_0 in models for infectious diseases in heterogeneous populations*, J. Math. Biol. 28 (1990), 365-382.

[4] P. van den Driessche and J. Watmough, *Reproduction numbers and subthreshold endemic equilibria for compartmental models of disease transmission*, Math. Biosci. 180 (2002), 29-48.

[5] P. van den Driessche and J. Watmough, *Further notes on the basic reproduction number*, in: F. Brauer et al (Eds), Mathematical Epidemiology, Lecture Notes in Mathematics, vol. 1945, Springer, New York, 2008, pp. 159-178.

[6] J. M. Heffernan, R. J. Smith and L. M. Wahl, *Perspectives on the basic reproductive ratio*, J. R. Soc. Interface, 2 (2005), 281-293.

[7] H. W. Hethcote, *The mathematics of infectious diseases*, SIAM Rev. 42 (2000), 599-653.

[8] S. Kim, Y. B. Seo and E. Jung, *Prediction of Covid-19 transmission dynamics using a mathematical model considering behavior changes in Korea*, Epidemiology and Health, 42 (2020), DOI: 10.4178/epih.e2020026.

[9] A. J. Kucharski, T. W. Russell, C. Diamond, Y. Liu, J. Edmunds, S. Funk and R. M. Eggo, *Early dynamics of transmission and control of COVID-19: a mathematical modelling study*, Lancet Infectious Diseases 2020, 20:553-558, DOI: 10.1016/S1473-3099(20)30144-4.

[10] S. A. Lauer, K. H. Grantz, Q. Bi, F. L. Jones, Q. Zheng, H. A. Meredith et al, *The incubation period of coronavirus disease 2019 (Covid-19) from publicly reported confirmed cases: estimation and application*, Ann. Intern. Med. 172 (2020), 577-582.

[11] Q. Li, X. Guan, P. Wu, L. Zhou et al., *Early transmission dynamics in Wuhan, China, of novel coronavirus-infected pneumonia*, New Engl. J. Med. 2020, 382:1199-1207, DOI: 10.1056/NEJMoa2001316.

[12] M. Martcheva, An Introduction to Mathematical Epidemiology, Springer, New York, 2015.

[13] A. Mellan, H. H. Hoeltgebaum, S. Mishra, C. Whittaker et al., *Estimating COVID-19 cases and reproduction number in Brazil*, Report # 21, Imperial College London, May/2020, DOI: 10.25561/78872.

[14] S. Vaid, C. Cakan and M. Bhandari, *Using machine learning to estimate unobserved COVID-19 infections in North America*, J. Bone Joint Surg. Am. 2020, 00:1-5 (DOI: 10.2106/JBJS.20.00715).